

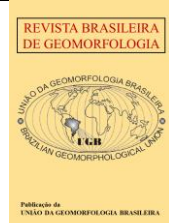


<https://rbgeomorfologia.org.br/rbg>
ISSN 2236-5664

Revista Brasileira de Geomorfologia

v. 23, n° 4 (2022)

<http://dx.doi.org/10.20502/rbg.v23i4.2183>



Research Article

Semi-automatic identification of Neogene deposits by using Digital Surface Model from high resolution images

Identificação semiautomática de depósitos neogênicos por meio de Modelos Digitais de Superfície obtidos de imagens de alta resolução espacial

Sonia Maria Lima Silva¹, Claudio Limeira Mello², Volker Hochschild³, José Duarte Correia⁴

¹ Departamento de Cartografia, FEN, Universidade Estadual do Rio de Janeiro (UERJ), Rio de Janeiro, Brasil.
sonia.silva@eng.uerj.br

ORCID: <https://orcid.org/0000-0002-2414-1516>

² Departamento de Geologia/IGEO/CCMN, Universidade Federal do Rio de Janeiro (UFRJ), Rio de Janeiro, RJ, Brasil.
limeira@geologia.ufrj.br

ORCID: <https://orcid.org/0000-0002-0456-3367>

³ Geoinformatik/Geographie/Mathematisch-Naturwissenschaftliche Fakultät - Universität Tübingen, Tübingen, Germany.
volker.hochschild@uni-tuebingen.de

⁴ Coordenação de População e Indicadores Sociais/DP – Instituto Brasileiro de Geografia e Estatística (IBGE), Rio de Janeiro, RJ, Brasil. jose.duarte.1958@gmail.com

ORCID: <https://orcid.org/0000-0003-2728-6750>

Received: 24/11/2021; Accepted: 27/06/2022; Published: 01/10/2022

Abstract: Cenozoic deposits occupy large areas of Brazilian territory and are little known or researched. The Barreiras Formation is one of the most important Cenozoic (Neogene) sedimentary units in Brazil and is associated with tabular landforms, dissected in deep valleys with steep slopes. This article proposes a semi-automatic methodology of mapping these deposits, in detailed scale, employing Digital Surface Models obtained from stereoscopic pairs of high resolutions satellite images. The methodology consisted of: (1) MDS and orthoimage generation, using an empirical model of rational functions and RPCs coefficients; (2) vertical and horizontal accuracy control; (3) DSM preparation; (4) terrain analysis and map generation from combining and interpreting morphometric variables; and (5) qualitative and quantitative evaluation of maps, using map algebra. The limits of the Barreiras Formation were identified by combining the following variables: height, slope, curvature and indices TRI, MRVBF and MRRTF. The results showed 83% correlation. From the percentage of uncorrelated areas, 9% presented false negatives and coincided with the areas of modified morphology due to uplift by tectonic movements. The proposed methodology proved to be fundamental for reducing the time for generating detailed scale maps.

Keywords: Cenozoic deposits; Barreiras Formation, DSM; orthoimage.

Resumo: Os depósitos cenozoicos ocupam grandes áreas do território brasileiro, sendo pouco conhecidos e pesquisados. A Formação Barreiras é uma das unidades sedimentares cenozoicas (Neógeno) mais importantes do Brasil, associando-se a relevo de formas tabulares, dissecadas em vales profundos com declives acentuados. Esse trabalho propõe uma metodologia semiautomática de mapeamento desses depósitos, em escala detalhada, empregando Modelos Digitais de Superfície obtidos de pares estereoscópicos de imagens de satélite de alta resolução. A metodologia consistiu em: (1) geração dos MDS e ortoimagens, usando modelo empírico de funções racionais e coeficientes RPC; (2) avaliação da precisão altimétrica e planimétrica; (3) preparação dos MDS; (4) análises de terreno e geração de mapas, a partir da combinação e interpretação de variáveis morfométricas; e (5) avaliação qualitativa e quantitativa dos mapas, por meio de álgebra de mapas. Os limites da Formação Barreiras foram identificados combinando as variáveis: altitude, declividade, curvatura e índices TRI, MRVBF e MRRTF. Os resultados do mapeamento apresentaram 83% de correlação. Do percentual de áreas não correlacionadas, 9% apresentaram falsos negativos e coincidiram com as áreas cuja morfologia foi alterada devido ao soerguimento por movimentos tectônicos. A metodologia proposta mostrou-se fundamental para redução do tempo na geração de mapas em escala de detalhe.

Palavras-chave: Depósitos cenozoicos, Formação Barreiras, MDS, ortoimagem.

1. Introduction

Cenozoic deposits occupy 32.4 % of the Brazilian continental surface (Bizzi *et al.*, 2003) and their areas are subject to intense occupation. Nevertheless, they still remain little known or researched.

The Barreiras Formation is an important Cenozoic sedimentary unit found along the Brazilian coast (Figure 1) and the term "Barreiras" refers to the coastal cliffs. Another remarkable geomorphologic characteristic related to the Barreiras Formation corresponds to a smooth and tabular hilly topography. This unit covers Precambrian rocks and Mesozoic onshore sedimentary rocks of several marginal basins and consists of interbedded layers of sandstones and mudstones deposited in fluvial and transitional environments, cemented by iron oxides/hydroxides (Morais *et al.*, 2006; Rossetti, 2006). The depositional time interval is estimated as Miocene to Pliocene (Bezerra *et al.*, 2006) and precedes the Quaternary deposits of the Brazilian coast.

The huge population concentrated on the coastal areas of Brazil has caused an intense and frequent exploitation of the Barreiras Formation, due to its abundance of raw minerals and its hydrological resources. This sedimentary unit is considered an important aquiferous reserve.

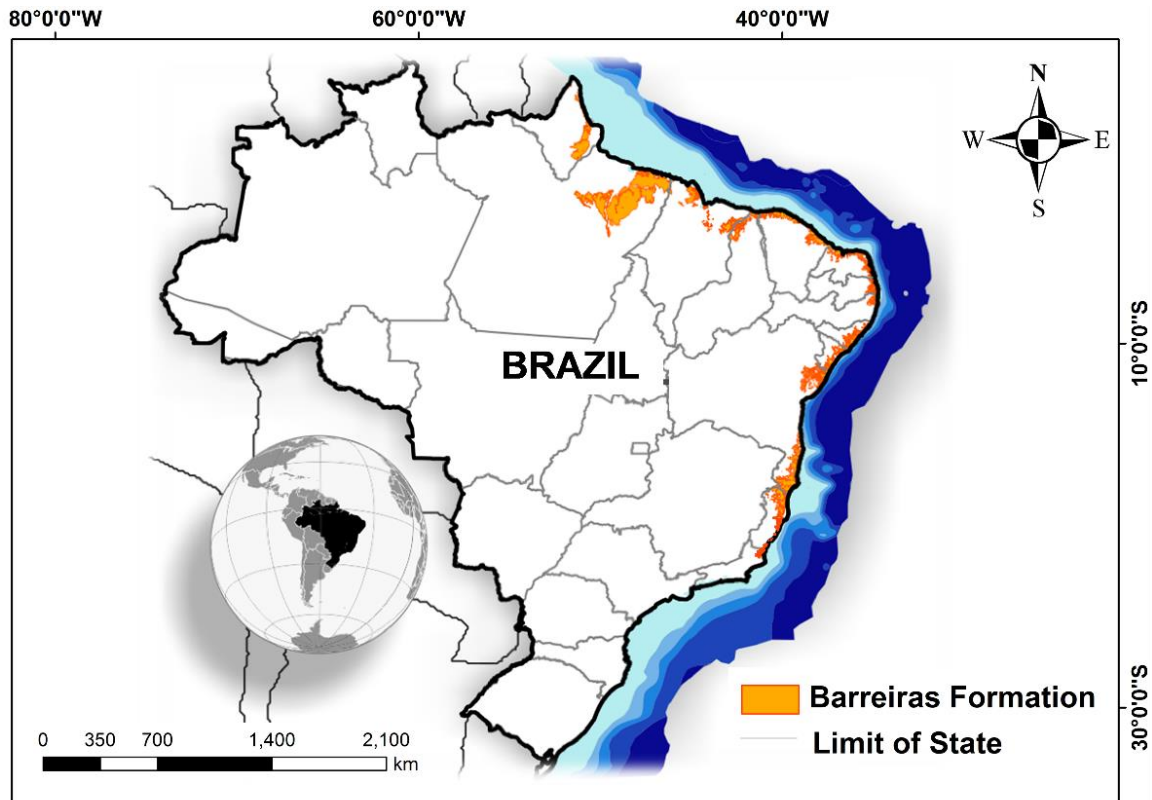


Figure 1. Distribution of the Barreiras Formation along the Brazilian coast. Source: Bizzi *et al.* (2003).

Several Cenozoic sedimentary units occur in a fragmented way throughout the eastern portion of Brazil. Despite of the absence of clear differentiation criteria for their identification, they were individualized in different stratigraphic units (Saadi *et al.*, 2005). Suguio & Nogueira (1999) pointed out that these sediments may be related to the sedimentation of the Barreiras Formation, which reinforces the need for further studies, including detailed mapping. Therefore, local analysis and regional correlations are essential for the reconstitution of Neogene events in Brazil.

The lack of topographic charts in appropriate scale makes the geological, geomorphological and pedological mapping in a detailed scale impossible. Currently in Brazil, in terms of cartographic maps used in the thematic mapping of a more detailed scale, one of the difficulties which arises is the fact that the country still does not have all the territory mapped in a scale greater than 1:100,000. Moreover, currently there are no geological maps of the Barreiras Formation on a larger scale than 1:250,000, which can provide greater detail about its occurrence. Its wide spatial distribution makes it difficult, time consuming and expensive to map the Barreiras Formation by using conventional methods (such as field surveys).

In this context and based on the hypothesis that the Barreiras Formation has typical geomorphological characteristics which can be identified through surface parameters, this article proposes a methodology for semi-automatic identification of this unit using geomorphometric analyses on Data Surface Models (DSM) generated from high resolution images. The orthoimagery generated by using the rational functions model, at a scale of about 1:25,000, will address the problem of the lack of geological maps of the Barreiras Formation at a more detailed scale. The challenge of mapping the Barreiras Formation lies in the fact that the action of weathering and tectonic deformation has altered its typical geomorphological characteristics.

2. The Study Area

This study was conducted in the northeast of the State of Rio de Janeiro, in Southeastern Brazil (Figure 2). The study area is approximately 1,225 km² and is located between the parallels 21°10'S and 21°35'S and meridians 41°05'W and 41°31'W. It contains the main occurrence of the Barreiras Formation deposits in the State of Rio de Janeiro.

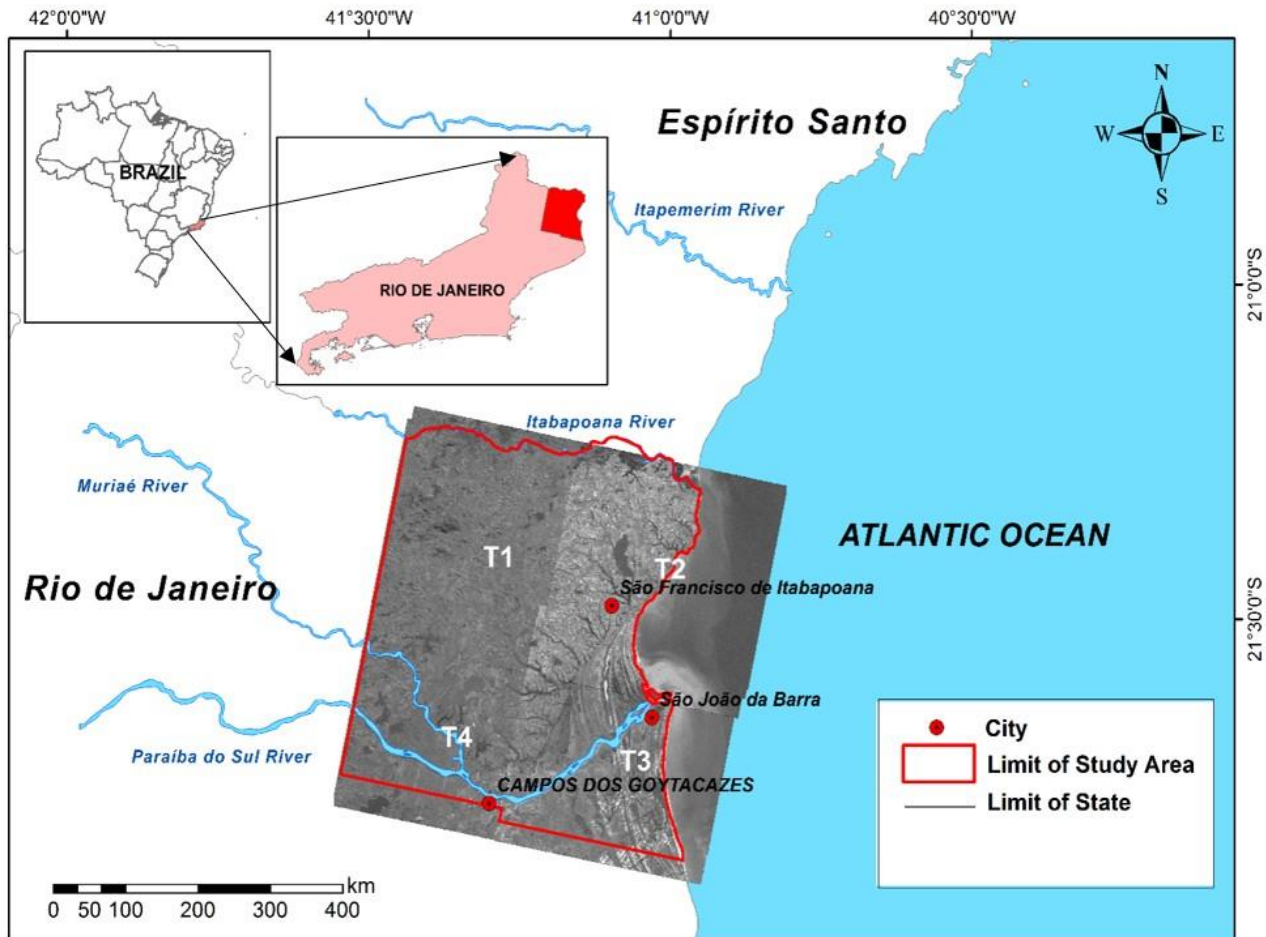


Figure 2. Study area covered by the four scenes (T1, T2, T3 and T4) from the ALOS/PRISM panchromatic sensor.

The regional geology is characterized by the occurrence of three major units: a Precambrian basement, the Barreiras Formation deposits and Quaternary sedimentary deposits (Martin et al., 1997).

The State of Rio de Janeiro, and thus the study area, is located in the Mantiqueira Province, one of the structural provinces defined by Almeida et al. (1981), formed in the late Neoproterozoic and early Paleozoic in the East and West Gondwana blocks (Heilbron et al., 2020). The Mantiqueira Province encompasses Araçuaí, Ribeira, Southern Brasília and Dom Feliciano orogenic belts. The State of Rio de Janeiro is located in the inner portion of the Ribeira orogenic belt (Almeida et al., 1973). In the study area, the Precambrian basement is formed by highly metamorphic (mainly gneiss and migmatites) and plutonic rocks (Silva & Cunha, 2001; Heilbron et al., 2016).

In the study area, the Cenozoic sediments of the Barreiras Formation overlie the crystalline basement and are formed by sandstones and mudstones related to a fluvial depositional system (Morais et al., 2006).

Martin et al. (1997) describes the Quaternary sedimentation as being formed by Pleistocene and Holocene marine terraces, Holocene lagoonal deposits and Holocene continental deposits.

The relief of the study area is quite varied, formed by mountains, hills, tablelands and a huge extent of

lowlands (floodplains and coastal zones with sand barriers). The existence of the mountains and hills is dating back to the Precambrian period, while the tablelands (associated with deposits of the Barreiras Formation) date from Miocene-Pliocene. The lowlands are more recent and date from Pleistocene to Holocene (Bidegain, 2002).

The available maps of the Barreiras Formation in the study area show remarkable divergences in the contact with the basement rocks (Figure 3). This fact shows the importance of using more precision data for an accurate identification of the deposits. On the other side, there are no significant differences between the maps in the contact of Barreiras Formation and the Quaternary deposits, most likely because it is easier to distinguish the two units.

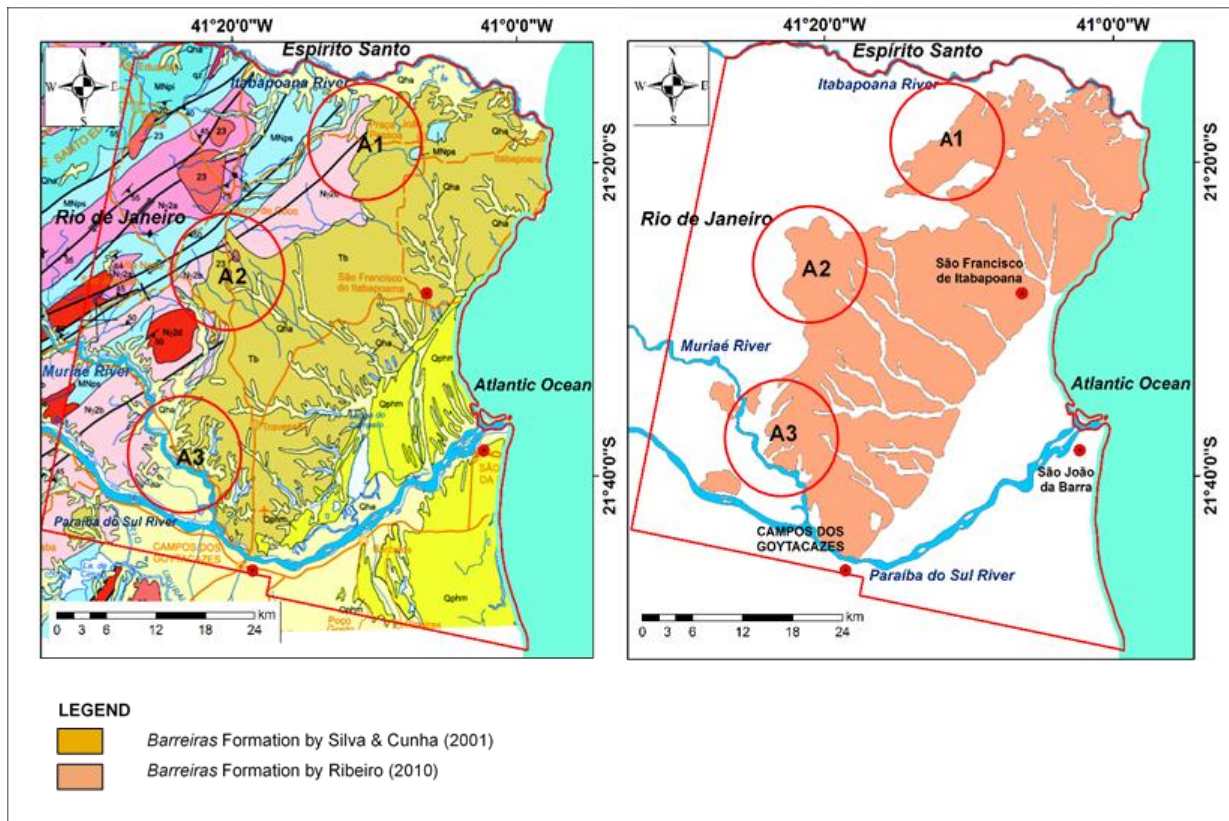


Figure 3. Examples of differences in contours of the Barreiras Formation in the study area: (a) Silva & Cunha (2001), from conventional geological mapping in the scale of 1:500,000; and (b) Ribeiro (2010), from visual interpretation on the SRTM DEM with 90 m resolution in the scale of 1:250,000. More significant differences are highlighted in the A1, A2 and A3 areas.

3. Material and Methods

3.1 Material

3.1.1 Data Sources

- Four stereoscopic scenes from the ALOS/PRISM satellite imagery, comprising 3 (three) high resolution images each scene (for viewing nadir, forward and backward). The panchromatic sensor is a radiometer sensor with 2.5m of spatial resolution at nadir. The images cover a width of 35km. The images have the 1B2R processing level. They have radiometric and geometric corrections and are georeferenced;
- Geological map from Silva & Cunha (2001);
- Geomorphological map from Dantas (2000);
- Thematic maps from Ribeiro (2010) and from Chrismann (2014); and

- Ground control points (GCPs) obtained from the Brazilian Institute of Geography and Statistics (IBGE).

3.1.2 Software

- PCI GEOMATICS v. 2010 and v. 2013 - The first version is available on NEQUAT/Department of Geography/UFRJ and the second one was made available for free by contacting PCI Geomatics;
- Leica Geosystems/Leica Photogrammetry Suite (LPS) v. 9.2. Available at the Institute of Geography/Universität Tübingen;
- Automated System for Geoscientific Analysis (SAGA) v. 2.0. Available for free at <http://www.saga-gis.org/>;
- ArcGIS Desktop v. 9.3 and v. 10.1, including three applications: ArcCatalog, ArcMap, and ArcToolbox. Available at NEQUAT/Department of Geography/UFRJ and at the Institute of Geography/Universität Tübingen;
- Mapgeo2010 v. 01. Available for free at www.ibge.gov.br;

3.2 Methods

The study was divided into five steps: (1) geometric and radiometric corrections; (2) vertical and horizontal accuracy assessment; (3) Digital Surface Model preparation; (4) terrain analysis and map generation; and (5) qualitative and quantitative evaluation of maps.

3.2.1 Geometric and radiometric corrections

The raw images often contain several geometric distortions and may not be directly integrated with other mapping products in a GIS environment, being necessary to apply either geometric as radiometric corrections, adapted to the nature and characteristics of image data (Toutin, 2004).

Although images from ALOS/PRISM sensor have specific problems of radiometric quality, which causes gross errors in the image, the results of sensor orientation and correlation have a good level of accuracy (Gruen et al., 2007).

For comparison purposes of the respective results, the geometric correction of images was conducted using two different software applications: PCI GEOMATICS and LPS.

Due to the reduced number of Ground Control Points (GCP), and availability of the Rational Polynomial Coefficients (RPC) data, provided with the images, the model for optical sensors using Rational functions was selected. Since this model does not require a prior information on any component of the total system (platform, sensor, Earth, map projection), it does not reflect the sources of image distortions (Toutin et al., 2002). However, according to Tommaselli and Medeiros (2010), the Rational Function model, using Rational Polynomial Coefficients (RPC), is used when the parameters of the acquisition system are not provided by the satellite.

The activities involved in the geometric correction were: (i) the creation of epipolar image pairs; (ii) the generation of the Digital Surface Model (DSM); and (iii) the geometric correction of the image itself.

The epipolar images were created for each stereoscopic pair: Backward-Nadir, Nadir-Forward and Backward-Forward, in order to reduce the search space and improve the matching process.

The DSM was computed by using the normalised cross-correlation method and the bilinear interpolator. The normalised cross-correlation method uses image correlation to search for homologous points in the

stereoscopic pair, being the method with the shortest processing time among those available. The bilinear interpolator uses the weighted average of the nearest eight pixels to determine the grey level of the pixel.

The interior and exterior orientation, as known in the classical Photogrammetry, were performed using the RPC data. By using the Rational Function model, the exterior orientation of the stereoscopic pair requires a single ground control point (GCP) (PCI, 2018). Even so, three control points were used to refine the exterior orientation. The accuracy of them was one third of the image resolution, as recommended by Merchant (1982).

Some computational applications offer smoothing functions for eliminating local noise and filling uncorrelated areas through interpolation based on the surrounding values (LPS, 2008; PCI, 2009b). The default options of filters were adopted in both software.

The DSM was generated with 10m resolution due to the terrain characteristics, the resolution of the image (2.5m) and the time spent for processing it.

The orthorectification was performed upon the nadir image of each scene. According to Meneses & Almeida (2012), the orthorectification must be performed upon the image with the lowest viewing angle, because the closer to the nadir, the less the image distortion.

3.2.2 Vertical and horizontal accuracy assessment

The quality control of the cartographic documents is done, in general, by means of point features, through their three-dimensional coordinates, obtained by topographic or geodetic surveys, or even from cartographic documents.

The evaluation of the positional quality of cartographic products, in Brazil, is based on the Standard of Cartographic Accuracy (PEC), established in Decree Law 89.817 of June 20, 1984 and created to assess digital cartographic products (BRAZIL, 1984). The classification of any cartographic document must meet, simultaneously, the PEC and EP (Standard Error) reference values available for different topographic scales.

The Table 1 and Table 2 show the standards values adopted in some scales of the Brazilian mapping system for vertical and horizontal accuracy, respectively. The vertical accuracy standard adopted in Brazil is based on both parameters: the one-dimensional linear error at the 90% confidence level (LE90) and the root mean square error (RMSE). Likewise, the horizontal accuracy standard adopted in Brazil is based on both parameters: the two-dimensional circular error at the 90% confidence level (CE90) and the root mean square error (RMSE) (Brazil, 1984).

Table 1. Standard values of the LE90 and vertical RMSE in some Brazilian system mapping scales.

Source: Brasil (1984).

Scale	Eq* (m)	Class					
		A		B		C	
		LE90 (m)	RMSE (m)	LE90 (m)	RMSE (m)	LE90 (m)	RMSE (m)
1:250,000	100	50.0	33.4	60.0	40.0	75.0	50.0
1:100,000	50	25.0	16.7	30.0	20.0	37.5	25.0
	40	20.0	13.4	24.0	16.0	30.0	20.0
1:50,000	20	10.0	6.7	12.0	8.0	15.0	10.0
1:25,000	10	5.0	3.4	6.0	4.0	7.5	5.0
1:10,000	5	2.5	1.7	3.0	2.0	3.8	2.5

* Equidistance of contour lines, existing values in the Brazilian system topographic mapping

Table 2. Standard values of the CE90 and horizontal RMSE in some Brazilian systematic mapping scales. Source: Brasil (1984).

Scale	Class					
	A		B		C	
	CE90 (m)	RMSE (m)	CE90 (m)	RMSE (m)	CE90 (m)	RMSE (m)
1:250,000	125.0	75.0	200.0	125.0	250.0	150.0
1:100,000	50.0	30.0	80.0	50.0	100.0	60.0
1:50,000	25.0	15.0	40.0	25.0	50.0	30.0
1:25,000	12.5	7.5	20.0	12.5	25.0	15.0
1:10,000	5.0	3.0	8.0	5.0	10.0	6.0

The Decree Law 89.817 considers the term "standard error" (EP) equivalent to the "root mean square error" (RMSE), sample estimator of the standard deviation, associated with the confidence level of 68.27% of the normal distribution of errors. The root mean square error (RMSE) is calculated using Eq. (1).

$$RMSE = \sqrt{\frac{\sum_{i=1}^n (l_i - l_v)^2}{n-1}} \tag{1}$$

Where l_i is the measurement performed, l_v , indicates the value taken as reference and n , the number of measurements performed.

The vertical error ve_i of each isolated point i of any cartographic document is calculated according to the Eq. (2).

$$ve_i = H_{di} - H_{ri} \tag{2}$$

Where H_{di} is the height of point obtained by interpolation in the cartographic document and H_{ri} , is the height of reference point.

The horizontal error he_i observed at each point i in terms of its UTM coordinates E and N, observed in the cartographic document being evaluated, compared to the respective coordinates taken as reference, is calculated by the Eq. (3).

$$he_i = \sqrt{(Eo_i - Ec_i)^2 + (No_i - Nc_i)^2} \tag{3}$$

Where, (Eo_i, No_i) are the UTM coordinates of points measured in cartographic document and (Ec_i, Nc_i) are the UTM coordinates of reference point.

The PEC value is associated with the interval centred on the mean of the observations with extremes distant from the mean of 1.6449 times the standard error or root mean square error, which corresponds to the 90% confidence level of the normal error distribution. The PEC value is calculated using Eq. (4).

$$PEC = 1,6449 * RMSE \tag{4}$$

The evaluation of vertical precision was performed by comparing the height values obtained in the DSM with the height of the reference points. The horizontal accuracy assessment was performed by comparing the

horizontal coordinates (E and N), obtained from the orthoimage, with their respective coordinates from the reference points.

The accuracy of the CGPs, used as vertical and horizontal reference, around 1m and 0.5m, respectively, were in accordance with the values established by Merchant (1982), who stated the values should be less than 1/3 of the technical standard value of RMSE.

3.2.3 Digital Surface Model preparation

The activities of DSM preparation included the identification and removal of spurious sinks or local depressions as well as their filtering. According to Wilson & Galant (2000), absolute measures of height errors do not provide a complete assessment of DSM quality, since most applications of DEMs depend on the representation of surface shape and drainage structure. Even if the automatic generation option is adopted, it is necessary some editions of the DSMs to adapt the model in water masses and the elimination of random errors.

While DSMs provide a detailed analytical description of the terrain, pixel-by-pixel, morphometric analysis is developed in a more regional context, requiring digital filter applications to smooth their surface and therefore generalise the information obtained (Correia, 2008). The low pass filters reduce what is known as high frequency noise (speckling), but they can also degrade some finer detail in the image, which renders it unfocused (Crósta, 1992).

Although filters were applied during the DSM generation process in order to eliminate noise, other low-pass filters were applied to prepare the DSMs for the subsequent phase of generating the geomorphometric variables

In order to compare the results, two low pass filters were selected: Gama filter (PCI Geomatics software) and the simple averaging technique FOCALMEAN (ArcGIS software).

The Gama filter can preserve some of the linear image features such as edges, filtering individual pixels in an image using the grey level values in a square window surrounding each pixel. Nevertheless, it does not permit to use window sizes larger than 11 by 11 pixels (PCI, 2009b). In contrast, the FOCALMEAN function allows the use of different sizes of moving windows to calculate the statistics. The filters were applied, varying the size of moving windows as well as the number of successive applications, in order to find out the appropriate number of iterations. The choice of the most suitable filter and the best combination of window size and number of iterations was made by evaluating the representation of three morphometric variables: height; slope; and curvature, derived from each smoothed DSM surface.

3.2.4 Terrain analysis and map generation

The terrain analyses included: (1) the generation of morphometric variables layers; (2) the classification and combination of layers; and (3) the generation of output maps.

- 1) The morphometric variables were generated using ArcGIS and SAGA software applications. The criteria for choosing the variables took into account the geomorphological aspects of the Barreiras Formation and the variables selected were: height, slope and curvature, highlighted by Mitasova & Hofierka (1993) as key elements to describe the terrain surface. In addition to these variables, the following morphometric indices were chosen: terrain roughness index (TRI); multiresolution index of valley bottom flatness (MRVBF); and multiresolution index of ridge top flatness (MRRTF).

Height refers to the variable that represents the distance measured along a perpendicular from one point on the ground surface and a reference surface (Maune *et al.*, 2001). As the Barreiras Formation deposits

outcrop at an intermediate height between the Quaternary and the basement, this variable becomes important in their identification when properly classified to reflect this height variation.

The slope corresponds to the rate of change of heights in the direction of steepest descent (Zevenbergen & Thorne, 1987; Wilson & Gallant, 2000). It is the first derivative of the height and is usually expressed in degrees, radians or percentages. Regions with little height variation, such as the large flat interfluves associated to the Barreiras Formation, must present slope values around zero.

The curvature is based on the second derivative of the height and measures the rate of slope change. It can be represented by two components: the profile and plan curvatures. The most common units of curvature are degrees, percentages, or radians per unit distance. In this research, the total curvature was considered, for achieving the best result in the identification of the Barreiras Formation. Moreover, considering the characteristic of flat tops of these deposits, the plan curvature would not bring any benefit, if analysed separately. The total curvature assumes positive or negative values, with zero curvature indicating that the surface is either flat or the convexity in one direction is balanced by the concavity in another direction (Wilson & Gallant, 2000). The flat tops of the Barreiras Formation should present values around zero.

The Terrain Roughness Index (TRI) is a quantitative measure of topographic heterogeneity of the terrain. In this research, the calculation of this index was performed using the function available in Morphometry module of SAGA software application, proposed by Riley et al. (1999). The method proposed by these authors employs the DoCELL function to calculate the sum of height differences between each pixel and its eight neighbours. As the Barreiras Formation presents small height variations, this index presented great potential to assist in its differentiation of basement domain.

The Multiresolution Index of Valley Bottom Flatness (MRVBF) is an index that can also be used to delineate hydrological and geomorphic units. The algorithm developed to calculate this index uses DEM to identify valley bottoms based on their topographic signature as flat low-lying areas. The algorithm uses slope and height to classify the degree of flattening of the valley bottoms. It operates at a range of scales (from coarser to finer resolutions) and combines the results at different scales into a single multiresolution index (Gallant & Dowling, 2003; Gallant et al., 2012). There is a routine within the same algorithm that generates the MRVBF, which identifies the tops of the hills and calculates the Multiresolution Index of Ridges Top Flatness (MRRTF). Both indices were calculated using the function available in the Morphometry module of the SAGA software application.

- 2) The layers of all morphometric variables were classified according to three classes representing: the basement; the Barreiras Formation; and the Quaternary plain, using the classified function of ArcGIS in the layer properties.

The combination of morphometric variables layers was done by using the ArcGIS/Spatial Analyst Tool/Combine function. The Combine function has a limitation in relation to the number of possible variables being combined simultaneously, on the order of twenty (ESRI, 2013c). This function assigns a single output value to each unique combination of input and records this value in the Value field of the attribute table. The output was a file, in raster format, containing integer values representing the three classes: the basement; the Barreiras Formation; and the Quaternary plain. In order to obtain a better representation of the Barreiras Formation deposits, several combinations of morphometric variables were tested, generating many output maps.

- 3) The output maps were created through generalisation process, aggregating cells based on the majority of their contiguous neighbouring. The generalisation process generating a more homogeneous representation of the Barreiras Formation deposits.

3.2.5 Quantitative and qualitative assessment of maps

The quantitative and qualitative assessment was performed by comparing the output maps, generated previously, with a reference map generated by Chrismann (2014) by using visual interpretation method (time consuming) on the DSM generated in this study, with 10 m resolution.

The quantitative assessment was done by using correlation analysis, comparing each output map with the reference map generated by Chrismann (2014). Subsequently, the map that presented the best correlation result was chosen for the subsequent phase of qualitative assessment.

The qualitative assessment was carried out in order to evaluate the gains in identifying the Barreiras Formation using the proposed semi-automatic methodology. The criteria used for this assessment took into consideration three areas (A1, A2 and A3, shown in the Figure 3), that presented discordance in the contours of the Barreiras Formation deposits with the basement. The three areas of the map, chosen in the quantitative analysis, were compared with their respective areas in the map generated by Chrismann (2014).

4. Results

4.1 Geometric and radiometric corrections and accuracy assessment

The good level of accuracy, verified by the excellent results of the correlation coefficients, lower or near 1 pixel, could be observed in almost all DSMs generated in the test phase with both software (PCI and LPS), confirming the exposed by Gruen et al. (2007). Most of the DSMs reached the mapping requirements of the scale of 1:25,000.

However, despite having excellent vertical accuracy, the DSMs generated with the LPS software presented several problems of noise, as shown in Figure 4a, that could compromise the morphometric analysis resulting in false interpretations. On the other hand, due to the superior quality in terms of noise of the DSM generated with PCI GEOMATICS software (Figure 4b), the respective DSMs for the 4 triplets (T1, T2, T3 and T4) were selected to the subsequent stages.

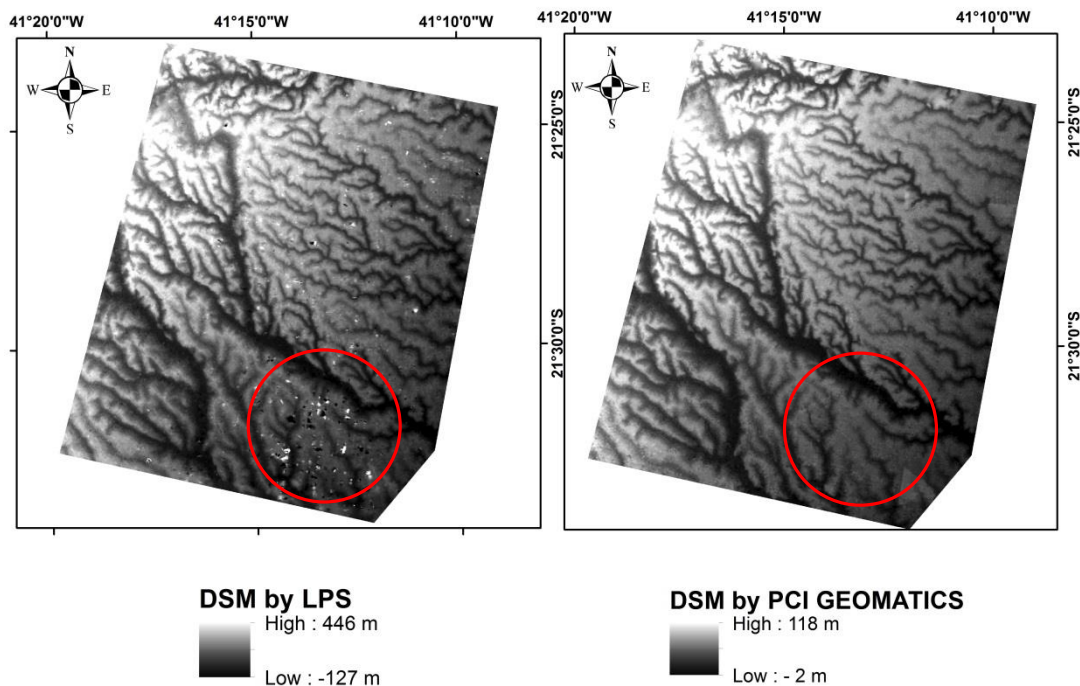


Figure 4. Detailed areas of: (a) DSM generated by LPS software and (b) DSM generated by PCI GEOMATICS software. Note the superior quality in terms of noise of the DSM generated with PCI GEOMATICS software.

The results of vertical accuracy assessment of the DSMs generated by PCI GEOMATICS software are presented in Table 3. For each triplet, the table 3 shows the LE90 and the RMSE values calculated from the DSMs and the technical standard values. Likewise, the results of horizontal accuracy assessment of the orthoimages generated by PCI GEOMATICS software are presented in Table 4. For each triplet, the table shows the CE90 and the RMSE values calculated from the orthoimages and the technical standard values. The excellent precision in results may be related to the quality of the DSMs, without noise, as well as the relief predominantly flat in the study area.

Table 3. Values of LE90 (Linear error at the 90% confidence level) and RMSE (Root Mean Square Error) of DSMs generated by PCI GEOMATICS software and the technical standards values for the scale of 1:25,000 Class A.

Triplet	Scale/ Class	DSMs		Technical Standards	
		LE90(m)	RMSE(m)	LE90(m)	RMSE(m)
T1	1:25,000/A	3.219	2.259	5.0	3.4
T2	1:25,000/A	3.642	2.234	5.0	3.4
T3	1:25,000/A	2.628	1.399	5.0	3.4
T4	1:25,000/A	3.184	1.968	5.0	3.4

Table 4. Values of CE90 (Circular Error at the 90% confidence level) and RMSE (Root Mean Square Error) of orthoimages generated by PCI GEOMATICS software and the respective technical standard values for the scale of 1:25,000 Class A.

Triplet	Scale/ Class	Orthoimages		Technical Standards	
		CE90(m)	RMSE(m)	CE90(m)	RMSE(m)
T1	1:25,000/A	7.683	2.083	12.5	7.5
T2	1:25,000/A	5.686	2.049	12.5	7.5
T3	1:25,000/A	6.152	2.582	12.5	7.5
T4	1:25,000/A	5.217	2.019	12.5	7.5

4.2 Terrain analysis and map generation

The value ranges that allowed the identification of the Barreiras Formation deposits, for three smoothed surfaces, are shown in Table 5. The intervals obtained from the three smoothed surfaces, with few exceptions, showed little variation. The selection of the best surface was conducted using as criterion the one that best identified the Barreiras Formation deposits, achieved by the surface smoothed 10 times with window size of 15 by 15 pixels. Therefore, the subsequent discussions will refer to this surface.

Table 5. Class intervals of morphometric variables of the Barreiras Formation for three smoothed surfaces obtained by using the averaging technique FOCALMEAN. Note that the smoothed surface of 15 by 15 pixels 10 times achieved the best result.

Morphometric variable	Smoothed surface	Smoothed surface	Smoothed surface
	15 by 15 pixels, 10 times	15 by 15 pixels, 14 times	21 by 21 pixels, 10 times
	Class Interval	Class Interval	Class Interval
	Barreiras	Barreiras	Barreiras
Height (m)	8.5 – 62.85	8.5 – 62.84	8.5 – 62.84
Slope (°)	0.15 – 3.26	0.15 – 2.5	0.15 - 2
Curvature (°/m)	-0.015 – 0.07	-0.01 – 0.04	-0.01 – 0.04
TRI (m)	0.015 – 0.4	0.02 – 0.35	0.02 – 0.3
MRVBF	0.8 - 7	0.9 – 7.93	1.35 - 8
MRRTF	0.38 – 9.87	0.35 – 9.87	0.38 – 9.53

4.3 Classification and combination of layers

Regarding the first variable (height), a clear increase of heights from SE to NW can be noticed. Height values at the boundaries between the Barreiras Formation and the Quaternary plain are characterized by abrupt changes and could be clearly identified. The boundary between the Barreiras Formation and the basement is less sharp and seems to be controlled by a NE-SW structure, confirming what was identified by Ribeiro (2010) on the predominance of structural pattern in this direction.

The results for the variables slope, curvature and the terrain roughness index (TRI) showed up very similar, allowing a relatively efficient distinction between the Barreiras Formation deposits and the Quaternary plain,

especially regarding the variables slope and TRI. In the areas of contact between the Barreiras Formation deposits and basement rocks, limits are less clear and the curvature seems more efficient.

The Multiresolution Index of Valley Bottom Flatness (MRVBF) showed better results in the distinction between the Barreiras Formation deposits and the Quaternary plain. One possible explanation is a greater flattening of the Quaternary areas, raising their classification level far above the valleys in the Barreiras Formation deposits. This index is not so efficient in distinguishing between the Barreiras Formation and the basement, which can be attributed to the fact that the valleys in the Barreiras deposits are increasingly less flattened and narrower as it approaches the contact with the basement.

The Multiresolution Index of Ridges Top Flatness (MRRTF) can be regarded as the less efficient variable in distinguishing between the Barreiras Formation deposits and the domains of the basement and the Quaternary plain. The distinction between the Barreiras Formation and the basement, based on the MRRTF index, is impaired due to the characteristically transitional morphology of the tops in the contact area. Regarding the distinction with Quaternary plain, this domain also presents very flattened morphology, similar to the tops of the Barreiras Formation deposits.

Normally, the complexity in the interpretation of results, obtained by using the combine function, is directly proportional to the number of variables used. In this study this was not a problem as the number of morphometric variables needed to represent the Barreiras Formation did not exceed this limit.

The results of the variable combination were strongly dependent on the quality of the previous classification.

4.4. Quantitative and qualitative assessment of maps

The best result of the quantitative analysis was obtained for the map combining the following variables: height, slope, curvature, TRI, MRVBF and MRRTF. This map presented the percentage values of correlated and uncorrelated areas of 83% and 17%, respectively. The correlated areas are equivalent to the sum of the areas related to Barreiras Formation and those which were not and the uncorrelated areas are equivalent to the sum of the false negatives and false positives (Figure 5).

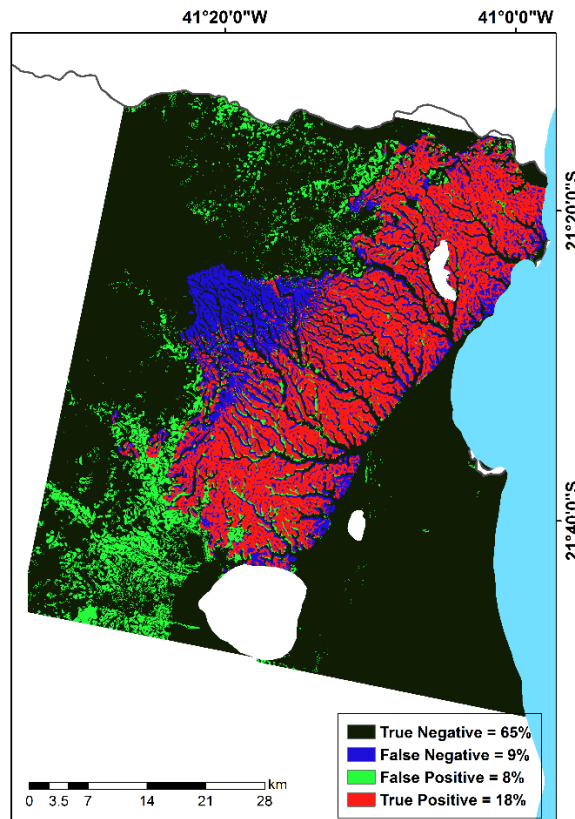


Figure 5. Results of the correlation analysis between the map generated with combinatorial OR method upon DSM smoothed surface 15 by 15 pixels, 10 times, using the morphometric variables: height, slope, curvature, TRI, MRVBF and MRRTF and the reference map generated by Chrismann (2014).

In the uncorrelated areas, the false negative of 9% was concentrated exactly upon the Barreiras Formation deposits which were uplifted due to tectonics, which is a very consistent result. Furthermore, the percentage of 8% of false positives was lesser when compared to other results.

The map generated in this study is presented in Figure 6 superimposed on the map generated by Chrismann (2014), used as a reference in the evaluation. The results show significantly more similarities than differences. An important similarity especially concerns the layout of the valleys that dissect the Barreiras Formation deposits. The biggest difference is in the A2 area, where the morphological characteristics of the Barreiras Formation deposits could not be verified due to neotectonic deformation appointed by Ribeiro (2010). Other differences are noted in the A1 and A3 areas near the contact with the basement, where the areas identified by the output map generated in this research are more extensive than those identified by Chrismann (2014).

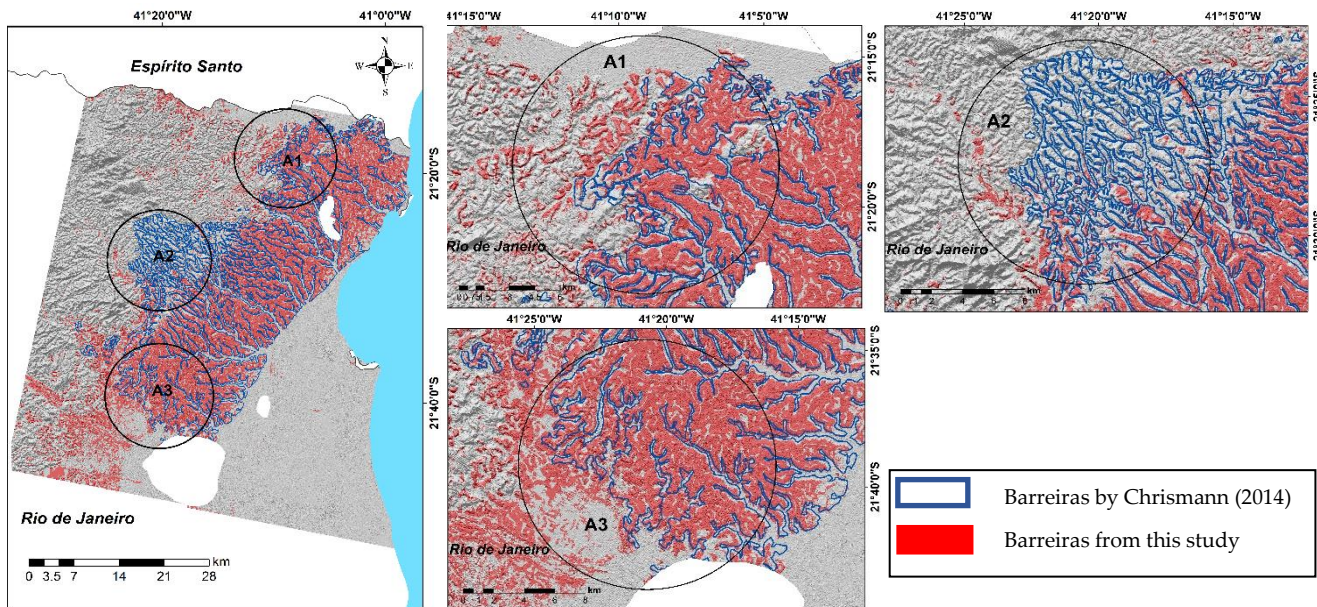


Figure 6. Comparison between the map of Barreiras Formation generated in this study and the map produced by Chrismann (2014). A1, A2 and A3 represent areas with discrepancies.

5. Conclusion

The main objective of this study, to successfully test a process of semi-automatic identification and detailed mapping of the Barreiras Formation deposits based on a morphometric analysis of digital surface models (DSMs) from high resolution optical satellite imagery, was achieved.

Regarding the methodology proposed in this study, it can be concluded that the rational function model reduced the number of ground control points (GCP) used for the generation of MDS and orthoimages and brought gains in time and cost for their acquisition. Moreover, the accuracy of the generated DSMs and orthoimages were compatible with the Brazilian Cartographic Standards for vertical and horizontal mapping in a scale of 1: 25,000 - Class A. It was proven that the processing and quality of the digital terrain model interfere directly in the results. The simple averaging technique FOCALMEAN to smooth the DSMs was adequate to attenuate the noise and also to generalize the morphometric variables information used in the regional analysis.

In relation to mapping, the best results for the identification of the Barreiras Formation, regarding their morphological characterization, were obtained with the combination of the following morphometric variables: 1. Height; 2. Slope; 3. Curvature; 4. terrain roughness index; 5. multiresolution index of valley bottom flatness; and 6. multiresolution index of ridge top flatness. The use of high resolutions images showed substantial gains in identifying the Barreiras Formation in terms of more detailed contour.

The methodology has provided the possibility to distinguish the Barreiras Formation from other regional geological units in other locations where the deposits present their usual morphological characteristics. Considering its wide spatial distribution in the Brazilian coastal region, the possibility of applying this methodology in other regions represents a gain in terms of time and costs compared to mapping by using the traditional field survey methods in detailed scale or even visual interpretation as the one done by Chrismann (2014).

Furthermore, this methodology can also be used to map other sedimentary geological units that have similar characteristics to the Barreiras Formation. This represents a significant gain for the methodology proposed.

Funding: this research was funded by Coordenação de Aperfeiçoamento de Pessoal de Nível Superior (CAPES).

Acknowledgments: the authors thank the Universidade Federal do Rio de Janeiro and Tübingen Universität for their institutional support, the Japan Aerospace Exploration Agency (JAXA), that provided the ALOS/PRISM images for free; Steven Corr and the entire support staff for providing the PCI Geomatics software licence and finally Mrs. Erin Skelton for the English revision.

Conflict of Interest: the authors declare that there is no conflict of interest.

References

1. ALMEIDA F.F.M de, AMARAL, G., CORDANI, H.G.; KAWASHITA, K. **The Precambrian evolution of South American cratonic margin, South of Amazon River.** In: A.E.M. Nairs & F.G. Stehli (Eds.), *The ocean basins and margins*. Plenum Press, New York: 411-446, 1973.
2. ALMEIDA, F.F.M. de, HASUI, Y., BRITO-NEVES, B.B de, FUCK, R. A. **Brazilian Structural Provinces: an introduction.** *Earth-Sci. Rev.*, 7817: 1-29, 1981.
3. BEZERRA, F.H.R., MELLO, C.L, SUGUIO, K. A. **Formação Barreiras: Recentes Avanços e Antigas Questões, Geologia USP (Série Científica), 6(2), Apresentação, 2006.**
4. BIDEGAIN, P. **Lagoas do Norte Fluminense – Perfil ambiental.** Secretaria de Estado de Meio Ambiente e Desenvolvimento Sustentável, Rio de Janeiro, 2002.
5. BIZZI, L. A., SCHOBENHAUS, C., VIDOTTI, R. M. et al. **Geologia, Tectônica e Recursos Minerais do Brasil: texto, mapas e SIG.** Brasília: CPRM, 674 p. il. 1 DVD anexo, 2003.
6. BRASIL, 1984. Decreto nº 89.817 de 20 de junho de 1984. Instruções Reguladoras das Normas Técnicas da Cartografia Nacional [online]. Diário Oficial da União. Brasília. Available in <http://www.concar.ibge.gov.br/indexf7a0.html?q=node/41>. Access on 10th Nov. 2013.
7. CHRISMANN, J. **Mapeamento da Formação Barreiras na Região Norte Fluminense, entre os Rios Paraíba do Sul e Itabapoana – Programa de Pós-Graduação em Geologia, UFRJ, Dissertação de Mestrado, 49 p., 2014.**
8. CORREIA, J.D. **Metodologia para Mapeamento Semi-Automático de Feições Depositionais Quaternárias por Imagens Orbitais de Alta Resolução Espacial : Médio Vale do Rio Paraíba do Sul - Programa de Pós-Graduação em Geologia, UFRJ, Tese de Doutorado, 665 p., 2008.**
9. CRÓSTA, A.P. **Processamento Digital de Imagens de Sensoriamento Remoto.** Campinas: IG/UNICAMP, 170 p., 1992.
10. DANTAS, M.E. Mapa geomorfológico do Estado do Rio de Janeiro. In: CPRM. *Geomorfologia do Estado do Rio de Janeiro*. Brasília: CPRM, 63. CD-ROM, 2000.
11. GRUEN, A.; KOCAMAN, S.; WOLFF, K. **Geometric Validation of ALOS/PRISM IMAGES.** ETH, Conference Paper, 2007.
12. HEILBRON, M., EIRADO, L.G., ALMEIDA, J. Mapa Geológico e de Recursos Minerais do Estado do Rio de Janeiro. Escala 1:400.000. Programa Geologia do Brasil (PGB). In: *Mapas Geológicos Estaduais*. CPRM-Serviço Geológico do Brasil, Superintendência Regional de Belo Horizonte, 2016, <http://geosgb.cprm.gov.br/>.
13. HEILBRON, M., VALERIANO, C. M., PEIXOTO, C., TUPINAMBÁ, M., NEUBAUER, F., DUSSIN, I., CORRALES, F., BRUNO, H., LOBATO, M., ALMEIDA, J. C. H. de, SILVA, L. G. E. **Neoproterozoic magmatic arc systems of the central Ribeira belt, SE-Brazil, in the context of the West-Gondwana pre-collisional history: A review** *Journal of South American Earth Sciences* 103(5):102710, 2020.

14. MARTIN, L., SUGUIO, K., DOMINGUES, J.M.L., FLEXOR, J.M. **Geologia do Quaternário costeiro do litoral norte do Rio de Janeiro e do Espírito Santo**. Belo Horizonte, CPRM, 112 p., 1997.
15. MENESES, P. R., & ALMEIDA T. D. **Introdução ao processamento de imagens de sensoriamento remoto** (1a ed.) Brasília: UNB, 2012.
16. MERCHANT, D. C. **Spatial accuracy standards for large scale line maps**. In: Technical Congress on Surveying and Mapping: Proceedings: V.1: 222-231, 1982.
17. MITASOVA, H.; HOFIERKA, J. Interpolation by regularized spline with tension. II. Application to terrain modeling and surface geometry analysis. **Mathematical Geology**, V. 25, n. 6, 1993, Available at:
18. <<http://skagit.meas.ncsu.edu/~helena/gmslab/papers/MG-II-93.pdf>>. Access on: 02 Dez. 2013.
19. MORAIS, R.M.O., MELLO, C.L., COSTA, F.O., SANTOS; P.F. Fácies Sedimentares e Ambientes Depositionais Associados aos Depósitos da Formação Barreiras no Estado do Rio de Janeiro, **Geologia USP (Série Científica)**, 6(2): 19-30, 2006.
20. PCI GEOMATICS. Focus User Guide - Version 10.3. Ontario, Canada: PCI Geomatics Enterprises, 2009b.
21. RIBEIRO, C. S. **Influência da Tectônica Pós-Deposicional na Distribuição da Formação Barreiras entre o Rio Paraíba do Sul (RJ) e o Rio Doce (ES) – Programa de Pós-Graduação em Geologia, UFRJ**, Dissertação de Mestrado, 165 p. , 2010.
22. ROSSETTI, D.F. Evolução Sedimentar Miocênica nos Estados do Pará e Maranhão. **Geologia USP (Série Científica)**, 6(2): 7-18, 2006.
23. SAAFI, A.; BEZERRA, F.H.R.; COSTA, R.D.; IGREJA, H.L.S.; FRANZINELLI, E. Neotectônica da plataforma brasileira. In: Souza, C.R.G.; Suguio, K.; Oliveira, A.M.S.; Oliveira, P.E. (eds) **Quaternário do Brasil**. Ribeirão Preto: Holos, Cap. 10: 211-234, 2005.
24. SILVA, L.C., CUNHA, H.C.S. **Geologia do Estado do Rio de Janeiro: texto explicativo do mapa geológico do Estado do Rio de Janeiro**. Brasília: CPRM, 2001.
25. SUGUIO, K.; NOGUEIRA, A.C.R. Revisão crítica dos conhecimentos geológicos sobre a Formação Barreiras do Neógeno e o seu possível significado como testemunho de alguns eventos geológicos mundiais. **Revista Geociências**, São Paulo, V. 18, n. 2: 461-479, 1999.
26. TOMMASELLI, A. M. G., & MEDEIROS, N. G. Determination of the indirect orientation of orbital images using control straight lines. **The Photogrammetric Record**, 25 (130): 159–179, 2010.
27. TOUTIN, T.; CHÉNIER, R.; CARBONNEAU, Y. 3D models for high resolution images: examples with QuickBird, Ikonos and Eros. In: ISPRS SYMPOSIUM. **Proceedings...** Ottawa, Canada, 8-12 July 2002. V. 43, part 4: 547-551, 2002.
28. TOUTIN, T. Review article: geometric processing of remote sensing images: models, algorithms and methods. **International Journal of Remote Sensing**, 25(10): 1893-1924, 2004.



Esta obra está licenciada com uma Licença Creative Commons Atribuição 4.0 Internacional (<http://creativecommons.org/licenses/by/4.0/>) – CC BY. Esta licença permite que outros distribuam, remixem, adaptem e criem a partir do seu trabalho, mesmo para fins comerciais, desde que lhe atribuam o devido crédito pela criação original.